Theoretical considerations about heavy-ion fusion in potential scattering

L. F. Canto,[1,2,*] R. Donangelo,[3,†] M. S. Hussein,[4,5,6,‡] P. Lotti,[7,§] J. Lubian,[2,‖] and J. Rangel[2,¶]

[1]*Instituto de Física, Universidade Federal do Rio de Janeiro, CP 68528, 21941-972, Rio de Janeiro, RJ, Brazil*
[2]*Instituto de Física, Universidade Federal Fluminense, Av. Litoranea s/n, Gragoatá, 24210-340, Niterói, RJ, Brazil*
[3]*Instituto de Física, Facultad de Ingeniería, Universidad de la República, C.C. 30, 11000 Montevideo, Uruguay*
[4]*Instituto de Física, Universidade de São Paulo, C.P. 66318, 05314-970, São Paulo, SP, Brazil*
[5]*Instituto de Estudos Avançados, Universidade de São Paulo, C.P. 72012, 05508-970, São Paulo, SP, Brazil*
[6]*Instituto Tecnológico de Aeronáutica, 12228-900, São José dos Campos, SP, Brazil*
[7]*INFN, Sezione di Padova, Via F. Marzolo 8, 35131, Padova, Italy*

(Received 18 May 2018; revised manuscript received 6 August 2018; published 22 October 2018)

We carefully compare the one-dimensional Wentzel, Kramers, Brillouin barrier tunneling model, and the one-channel Schrödinger equation with a complex optical potential calculation of heavy-ion fusion, for a light and a heavy system. It is found that the major difference between the two approaches occurs around the critical energy, above which the effective potential for the grazing angular momentum ceases to exhibit a pocket. The value of this critical energy is shown to be strongly dependent on the nuclear potential at short distances, on the inner region of the Coulomb barrier, and this dependence is much more important for heavy systems. Therefore the nuclear fusion process is expected to provide information on the nuclear potential in this region. We compare calculations with available data to show that the results are consistent with this expectation.

DOI: 10.1103/PhysRevC.98.044617

I. INTRODUCTION

Nuclear collisions involve several degrees of freedom. Besides the projectile-target separation vector, **r**, the collision depends on intrinsic coordinates of the collision partners, which are coupled with **r** by Coulomb and nuclear forces [1–4]. In this way, the collision may lead to various final states of the systems (channels). In addition to elastic scattering, it may undergo direct reactions, such as inelastic scattering, transfer and breakup, or fuse to form a compound nucleus (CN). The simplest quantum mechanical treatment of a nuclear collision, referred to as potential scattering, ignores all intrinsic degrees of freedom. It approximates the problem by a collision of two point particles, interacting through a real potential, $V(\mathbf{r})$. Clearly, this approach can only make predictions for elastic scattering. However, it is necessary to take into account the attenuation of the incident wave, resulting from transitions to nonelastic channels. Owing to these transitions, the current associated with the elastic wave function does not satisfy the continuity equation. This would be inconsistent with the wave function of a Hermitian Hamiltonian. To fix this problem, one simulates the effects of nonelastic channels by the inclusion of a negative imaginary part in the potential.

However, potential scattering is a very poor treatment of nucleus-nucleus collisions. More satisfactory results can be obtained through the coupled-channel (CC) approach. In this method, the wave function is expanded over a set of intrinsic states of the system and the expansion is inserted into the Schrödinger equation with the full Hamiltonian. In this way, one gets a set of coupled equations for the wave functions in these channels. If the expansion contained all relevant channels, one would obtain realistic predictions for the experimental cross sections. However, this condition is not satisfied in heavy-ion collisions, owing to the fusion channel. The formation of a compound nucleus and its subsequent decay are very complicated processes, which cannot be handled in the coupled-channel approach. Nevertheless, fusion and its influence on direct reactions must be taken into account. They can be estimated through the inclusion of an imaginary potential in the Hamiltonian. This potential must be negative and very strong to absorb completely the current that reaches the inner region of the Coulomb barrier. It is believed that the details of this potential are not important, provided that it produces strong short-range absorption.

An alternative way to handle fusion, is to keep the potential real and solve the radial equations with ingoing wave boundary conditions (IWBCs) at some radial distance $r = R_{\rm in}$, located in the inner region of the barrier. This procedure is adopted by some authors, and used in the CCFULL [5] computer code. The IWBC assumes that there are no reflected waves at $R_{\rm in}$, which implies that the incident wave is completely absorbed at $r < R_{\rm in}$. Thus, it is expected to be equivalent to solving the radial equation with the usual boundary conditions at $r = 0$, but with a complex potential, which produces total absorption in this region, and is not active elsewhere.

*canto@if.ufrj.br
†donangel@fing.edu.uy
‡hussein@if.usp.br
§paolo.lotti@pd.infn.it
‖lubian@if.uff.br
¶jeannie@if.uff.br

The purpose of the present work is to investigate the dependence of the fusion cross section on reasonable choices of the interaction. For simplicity, our study is restricted to potential scattering with real nuclear potentials evaluated by some version of the folding model. These potentials take into account the nuclear densities but ignores the nuclear structure properties of the collision partners. It is well known that these properties may strongly affect sub-barrier fusion. Therefore, we consider only collisions at above-barrier energies, where the fusion cross section predicted by potential scattering and the ones obtained in coupled-channel calculations are similar. Although this may not happen in fusion reactions with weakly bound projectiles, it does not affect our conclusions, since collisions of this kind are not considered here.

The paper is organized as follows. In Sec. II, we discuss the basic aspects of fusion in potential scattering within the Feshbach general description of nuclear reactions. In Sec. III we investigate the influence of different commonly used treatments of absorption and choices of the nuclear potential on the fusion cross section, considering as examples the cases of a heavy and a light system. Finally, in Sec. IV we present the conclusions of our work.

II. POTENTIAL SCATTERING WITHIN FESHBACH'S THEORY OF NUCLEAR REACTIONS

Commonly, the analyses of experimental nuclear scattering data are based on the use of the complex potential in potential scattering theory. The determination of the complex nuclear potential, referred to as the optical potential, is done by fitting the data of the elastic cross sections. For the sake of completeness we supply below the basic theory of the optical potential within the unified theory of Feshbach [6,7], which is based on many-body scattering theory.

In Feshbach's theory, the dynamics is governed by the full Hamiltonian of the system, $\mathbb{H}$, (blackboard bold fonts denote operators acting on both collision and intrinsic degrees of freedom),

$$\mathbb{H} = K + h + \mathbb{V}. \tag{1}$$

Above, K is the kinetic energy operator, h is the intrinsic Hamiltonian of the system, and $\mathbb{V}$ is the operator representing the interaction between the projectile and the target. This interaction depends both on the collision coordinate and the intrinsic degrees of freedom. The full scattering state is then the solution of the Schrödinger equation

$$[E - \mathbb{H}]\,|\Psi^{(+)}\rangle = 0, \tag{2}$$

with scattering boundary conditions.

The derivation of the optical potential can be made formally but quite transparently within the Feshbach theory. Denoting by P the elastic channel projection operator and by Q the projector on all other channels, both closed and open, one can decompose Eq. (2) into the coupled equations

$$[E - \mathbb{H}_{\rm PP}]\,|\Psi_{\rm P}^{(+)}\rangle = \mathbb{H}_{\rm PQ}\,|\Psi_{\rm Q}\rangle \tag{3}$$

$$[E - \mathbb{H}_{\rm QQ}]\,|\Psi_{\rm Q}\rangle = \mathbb{H}_{\rm QP}\,|\Psi_{\rm P}\rangle. \tag{4}$$

Above, we adopted the short-range notations: $\mathbb{H}_{\rm AB} = A\mathbb{H}B$, where A and B stand for any of the two projectors, $\Psi_{\rm P}^{(+)} = P\Psi^{(+)}$ and $\Psi_{\rm Q} = Q\Psi^{(+)}$. At this stage, we assume that only closed channels (compound nucleus) are coupled to the elastic channel.

Solving Eq. (4) for $\Psi_{\rm Q}$ and inserting the result into Eq. (3), we obtain the equation for the elastic component of the wave function,

$$[E - K - \mathbb{V}_{\rm PP} - \mathbb{V}_{\rm eff}]|\Psi_{\rm P}^{(+)}\rangle = 0, \tag{5}$$

where $\mathbb{V}_{\rm PP} = P\mathbb{V}P$. This equation involves the potential constrained to the subspace of the elastic channel, $\mathbb{V}_{\rm PP}$, plus the additional term

$$\mathbb{V}_{\rm eff} = \mathbb{H}_{\rm PQ}\,\frac{1}{E - \mathbb{H}_{\rm QQ}}\,\mathbb{H}_{\rm QP}. \tag{6}$$

The projectors can be expressed in terms of the eigenfunctions of h. Denoting them by $|\varphi_\alpha\rangle$, with $|\varphi_0\rangle$ standing for the ground state, they are given by

$$P = |\varphi_0)\,(\varphi_0|; \quad Q = \sum_{\alpha\neq 0} |\varphi_\alpha)\,(\varphi_\alpha|. \tag{7}$$

Inserting the above equations into Eq. (5), one gets the Schrödinger equation for potential scattering,

$$[E - K - \bar{U} - V_{\rm eff}]|\psi^{(+)}\rangle = 0, \tag{8}$$

where, $|\psi^{(+)}\rangle$ is the scattering state in the space of the collision degrees of freedom. Above,

$$\bar{U} = (\varphi_0|\,\mathbb{V}\,|\varphi_0) \tag{9}$$

represents the bare potential operator and

$$V_{\rm eff} = (\varphi_0|\,\mathbb{H}_{\rm PQ}\,\frac{1}{E - \mathbb{H}_{\rm QQ}}\,\mathbb{H}_{\rm QP}\,|\varphi_0) \tag{10}$$

is the effective compound nucleus coupling potential operator. Both $\bar{U}$ and $V_{\rm eff}$ are operators acting exclusively on the **r** space.

A. Bare potential

The potential $\bar{U}(r)$ of Eq. (9) is clearly real. It represents the interaction between the collision partners when they are in their ground states, that is, when couplings to nonelastic channels are completely ignored. It can be written as

$$\bar{U}(r) = U_{\rm C}(r) + \bar{U}_{\rm N}(r), \tag{11}$$

where $U_{\rm C}$ and $\bar{U}_{\rm N}$ are, respectively, the Coulomb and nuclear components of $\bar{U}$.

Adopting a microscopic point of view, where the intrinsic degrees of freedom are the nucleon coordinates, the bare potential in the coordinate representation can be evaluated by the folding model. Then, neglecting nucleon exchange, one gets

$$\bar{U}_{\rm N}(\mathbf{r}) = \int d\mathbf{r}'\,d\mathbf{r}''\;\rho_{\rm P}(\mathbf{r}')\,v(\mathbf{r} - \mathbf{r}' + \mathbf{r}'')\,\rho_{\rm T}(\mathbf{r}''). \tag{12}$$

Above, $\rho_{\rm P}$ and $\rho_{\rm T}$ are, respectively, the densities of the projectile and the target, and v is a conveniently chosen nucleon-nucleon interaction. A frequent trend in the literature

is to adopt Michigan's M3Y nucleon-nucleon interaction [8]. We consider two versions of the folding potential: The São Paulo potential (SPP) [9–11] and the Akyüz-Winther potential (AW) [12,13]. The SPP has two advantages. The first is that it restores, in an approximate way, exchange effects neglected in the folding integral. The second is that the authors developed a computer code to evaluate the integral of Eq. (12) using the most realistic densities available in the literature. On the other hand, there is the disadvantage that this code has not been published, and therefore it is not widely available. The AW potential has the disadvantage of being less accurate. It was developed in three steps. First, the authors used approximate analytical expressions for the densities, to simplify the folding integral. Second, they evaluated the potential for a large number of systems in different mass ranges, and fitted the potentials by WS functions. The fits aimed at reproducing the potential in the barrier region. Finally, they obtained approximate analytical expressions for the WS parameters, in terms of the mass numbers of the collision partners. In this way, the evaluation of the WS potential is extremely simple. Despite their different origins, the barriers of the SPP and the AW potential are quite similar. This point will be discussed further in Sec. III B.

B. Effective compound nucleus coupling potential

Now we consider the effective potential of Eq. (10), which accounts for the influence of CN couplings on the elastic wave function. The most important consequence of these couplings is the partial absorption of the incident wave, associated with the populations of CN states. The potential of Eq. (6) is real. Furthermore, this potential has poles at $E = \mathbb{H}_{QQ}$. This very strong energy dependence of the effective potential renders Eq. (10) useless.

The above-mentioned shortcomings can be eliminated through energy averaging. One chooses an interval in energy, I, which encompasses many compound nucleus resonances. This procedure leads to the complex potential [2,4,6,7,14],

$$V_{\rm eff} = (\varphi_0|\,\mathbb{H}_{PQ}\,\frac{1}{E-\mathbb{H}_{QQ}+iI/2}\,\mathbb{H}_{QP}\,|\varphi_0). \tag{13}$$

This potential can be written as

$$\mathbb{V}_{\rm eff} = \Delta U + i\,W. \tag{14}$$

The real part of $\mathbb{V}_{\rm eff}$,

$$\Delta U = (\varphi_0|\,\mathbb{H}_{PQ}\,\mathcal{P}\left\{\frac{1}{E-\mathbb{H}_{QQ}+iI/2}\right\}\mathbb{H}_{QP}\,|\varphi_0), \tag{15}$$

with $\mathcal{P}$ standing for the principal value, is a small correction to the potential $\bar{U}$ of Eq. (9). It is usually neglected.

On the other hand, the imaginary part of $\mathbb{V}_{\rm eff}$,

$$W = -\pi\,(\varphi_0|\,\mathbb{H}_{PQ}\left[\frac{I/2}{\left(E-\mathbb{H}_{QQ}\right)^2+I^2/4}\right]\mathbb{H}_{QP}\,|\varphi_0), \tag{16}$$

is very important. It is responsible for strong absorption of the low partial waves, as it will be discussed in detail below.

Equation (16) can be further reduced by using a spectral expansion of $\mathbb{H}_{QQ}$,

$$\mathbb{H}_{QQ}\,|q\rangle = \varepsilon_q\,|q\rangle.$$

One gets

$$W = -\frac{\pi\,I}{2}\sum_q \frac{(\varphi_0|\mathbb{V}\,|q\rangle\,\langle\tilde{q}|\,\mathbb{V}\,|\varphi_0)}{(E-\epsilon_q)^2+I^2/4}. \tag{17}$$

The above potential can be approximately evaluated through the following procedures. First, the q sum is replaced by an integral over ϵ_q, by introducing the density of states of the CN, $\rho_{\rm CN}(\epsilon_q)$. That is

$$\sum_q \to \int d\epsilon_q\;\rho_{\rm CN}(\epsilon_q). \tag{18}$$

The second step is to assume that this density is a slowly varying function of ϵ_q, and take it outside the integral. Then the ϵ_q integral is just the Lorentzian average of $(\varphi_0|\mathbb{V}|q\rangle\,\langle\tilde{q}|\mathbb{V}|\varphi_0\rangle$. The final approximate expression of the energy-averaged absorptive potential is

$$W = -2\pi\;\overline{\rho_q(\epsilon_q)\,(\varphi_0|\mathbb{V}|q\rangle\,\langle\tilde{q}|\mathbb{V}|\varphi_0\rangle}. \tag{19}$$

1. Digression into the Hauser-Feshbach compound nucleus model

It is important to mention that the introduction of energy averaging and the subsequent emergence of a complex interaction would seemingly violate flux conservation. However, this is fixed by tracking the path of the lost flux, which goes into the formation of the compound nucleus and separately calculate the decay of the latter using the so-called statistical theory. The corresponding cross section, the Hauser-Feshbach [15] cross section contribution to elastic scattering (compound elastic), is then added incoherently to the elastic cross section given by the Schrödinger equation with the optical potential. This potential includes an imaginary part corresponding to the local approximation to Eq. (19). In this way, the flux is accounted for completely.

Accordingly, if a comparison with the elastic scattering angular distribution or excitation function data is called for, then the theoretical cross section would, according to our discussion above, be composed of the optical potential contribution to the cross section plus the compound nucleus (Hauser-Feshabach) contribution. Interference terms can be made to average out to zero upon appropriate energy averaging as was demonstrated by Ref. [16]. In this way, the elastic cross section is given by

$$\sigma_{\rm el}(\theta) = \sigma_{\rm el}^{\rm opt}(\theta) + \sigma_{\rm el}^{\rm CN}(\theta), \tag{20}$$

where $\sigma_{\rm el}^{\rm opt}(\theta)$ is the elastic cross section calculated in potential scattering with the optical potential

$$V_{\rm opt} = \bar{U} + \Delta U + i\,W \tag{21}$$

and $\sigma_{\rm el}^{\rm CN}(\theta)$ is the Hauser-Feshbach contribution, arising from the decay of the CN through the elastic channel. It is given by

$$\sigma_{\rm el}^{\rm CN}(\theta) = \sum_l \sigma_{0,l}(\theta) \tag{22}$$

with

$$\sigma_{0,l}(\theta) = w\frac{\pi}{k_0^2}(2l+1)\frac{[\mathcal{T}_0(l)]^2}{\sum_\beta \mathcal{T}_\beta(l)}, \tag{23}$$

where k_0 is the wave number in the elastic channel. Above, $\mathcal{T}_\beta(l)$ is the transmission coefficient through the Coulomb barrier of the potential in a collision initiated in channel β. It is given by

$$\mathcal{T}_\beta(l) = 1 - |S_\beta(l)|^2, \tag{24}$$

where $S_\beta(l)$ is the lth component of the S matrix of an optical model calculation for channel β. The sum in the denominator of Eq. (23) runs over all decay channels of the CN.

The factor w in Eq. (23) is called the width fluctuation correction [17] or elastic enhancement factor [16,18]. This factor, which varies with the strength of absorption, starts with the value 3 when the resonances of the compound nucleus are isolated, which is the case at very low excitation energies [16,18], and attains the value of 2 when the compound resonances are overlapping (strong absorption). An experimental verification of the strong absorption limit, $w = 2$, was clearly demonstrated in the reaction ^{30}Si(p, p) at $E_p = 9.8$ MeV [19]. The values of w in the intermediate absorption region (weakly overlapping compound resonances) were calculated in Ref. [20] and were found to be in the range $2 < w < 3$, as announced above. Since the sum over decay channels in Eq. (23) can be large, the contribution of the compound elastic cross section Eq. (23) is usually small except for light heavy-ion systems.

The contribution from the CN to any nonelastic channel, say α, can be evaluated similarly. It is given by Eqs. (22) and (23), replacing in the numerator of the latter: $[\mathcal{T}_0(l)]^2 \to \mathcal{T}_\alpha(l)\,\mathcal{T}_0(l)$. Eqs. (22) and (23) then become

$$\sigma_\alpha^{\rm CN}(\theta) = \sum_l \sigma_{\alpha,l}(\theta), \tag{25}$$

$$\sigma_{\alpha,l}(\theta) = \frac{\pi}{k_0^2}(2l+1)\frac{\mathcal{T}_\alpha(l)\,\mathcal{T}_0(l)}{\sum_\beta \mathcal{T}_\beta(l)}. \tag{26}$$

Note that there is no nonelastic enhancement factor [16]. This suggests writing the general form of the compound nucleus cross section for a transition $0 \to \alpha$ as,

$$\sigma_{\alpha,l}(\theta) = \frac{\pi}{k_0^2}(2l+1)[1 + (w-1)\delta_{\alpha,0}]\frac{\mathcal{T}_\alpha(l)\,\mathcal{T}_0(l)}{\sum_\beta \mathcal{T}_\beta(l)}, \tag{27}$$

which reduces to Eq. (23) for the compound elastic case [18,20].

The fusion cross section is obtained by summing the Hauser-Feshbach cross sections of Eqs. (25) and (26) over all final decay channels of the CN (neutron, γ, elastic, inelastic, etc.). One gets the compound nucleus formation (fusion) cross section

$$\sigma_{\rm F} = \frac{\pi}{k_0^2}\sum_l (2l+1)\,\mathcal{T}_0(l). \tag{28}$$

The fusion transmission coefficient, $\mathcal{T}_0(l)$, is calculated directly from the optical potential Schrödinger equation, and multiplied by the compound nucleus formation probability as discussed below. Experimentally one measures evaporation channels of the compound nucleus and sums their contributions. If this sum is close to complete, then the fusion cross section is extracted and compared to one of the theoretical models, guided by the Hauser-Feshbach theory.

2. *Local version of the absorptive CN coupling potential*

Of course it is a long path to render the operator W of Eq. (19) into a potential that can be used in the one-channel optical potential Schrödinger equation. To begin with, the potential operator of Eq. (19) is nonlocal when written in configuration space. Secondly, it is potentially energy dependent. However, using the above discussion as a guide, it is customary to use a locally equivalent version of it, $W(r)$.

Although we are not aware of any formal proof that the imaginary potentials arising from couplings with CN states have a short range, they are expected to have this property, as a consequence of the confined nature of the states $|q\rangle$ appearing in Eq. (19). On the other hand, there is empirical evidence of it. Potential scattering studies of fusion [21] and CC calculations of fusion, elastic scattering and other reaction channels systematically adopt strong imaginary potentials with a short range to account for the fusion process [22,23]. Typical calculations adopt imaginary potentials with WS shapes with parameters of the order $W_0 \sim 50$ MeV, $r_0 \sim 1.0$ fm and $a \sim 0.2$ fm.

The above discussion clearly indicates that reference to the compound nucleus formed in the fusion process is important. Further, $W(r)$ may account for both closed channels (fusion) absorption and open channels ones (direct reactions). Of course these direct channels are accounted for in the Feshbach theory by allowing some of the Q-projected channels to be open ones.

3. *Contribution of direct channels*

It should be mentioned that the real part of the optical potential is given by the bare potential of Eq. (9) plus the correction ΔU [Eq. (15)]. When the couplings are restricted to CN states, this correction is negligible and the imaginary part W is very strong. When written in the configuration space, it is, as mentioned before, nonlocal. But a local version is constructed and its range is short.

The situation is different when couplings with open channels are taken into account. Then, the projector Q is split into two terms, one projecting onto closed, compound nucleus, channels and the other projecting onto open, direct ones. These direct channels include, among others, the breakup channel and in particular nonelastic breakup ones which contain incomplete fusion as an important absorptive effect in the case of light weakly bound projectiles, such as ^{6}Li $(=d + {}^4\text{He})$. Following the same procedures as in the case of purely closed channels, one gets an additional potential, usually called the polarization potential and denoted by $V_{\rm pol}$. Generally, $V_{\rm pol}$ is difficult to calculate except for some simple models of the structure of the target nucleus, such as highly deformed ones where a rotor model is employed. More realistic polarization potentials can be derived using wave functions obtained from CC calculations [24].

On the other hand, one can adopt a phenomenological approach to take into account average effects of both the CN and direct channels. It consists in using an imaginary potential with a longer range, reaching the surface region. Good descriptions of the elastic scattering and total reaction data have been achieved with an imaginary potential having the same shape as the real potential but with a slightly weaker strength [25]. However, this procedure fails when the couplings with open channels are very strong, as in collisions of a heavy projectile with a highly deformed target, or collisions of weakly bound systems.

C. One-channel description of absorption

Within a one-channel description, the elastic scattering and total reaction cross sections can be obtained solving the Schrödinger equation with the complex potential

$$V(r) = V_{\rm opt}(r) + V_{\rm pol}(r). \tag{29}$$

The scattering wave function, $\psi^{(+)}(\mathbf{r})$ is then calculated and the total reaction cross section, which is equal to the absorption cross section, is given by

$$\sigma_{\rm R} = \sigma_{\rm abs} = \frac{k}{E}\,\langle\psi^{(+)}| - {\rm Im}\{V\}|\psi^{(+)}\rangle. \tag{30}$$

The calculation of the fusion cross section is more complicated. One might be tempted to evaluate $\sigma_{\rm F}$ using the above expression, but with the replacement: ${\rm Im}\{V\} \to {\rm Im}\{V_{\rm opt}\}$. However this is not correct. The reason is that fusion can take place in the elastic channel and also in the direct channels associated with the potential $V_{\rm pol}$. The contributions from the nonelastic channels, which are quite important, would be completely ignored in this procedure. Then, it is better to evaluate the wave function using only the real part of the polarization potential, or to neglect it completely. At subbarrier energies, the real part of the polarization potential tends to reduce the Coulomb barrier, which enhances fusion. At above barrier energies, couplings with direct channels are not very important, except in some particular situations, such as complete fusion of weakly bound nuclei. Since we are mainly concerned with fusion cross sections above the Coulomb barrier, we will neglect polarization potentials in what follows.

If the optical potential accounts exclusively for couplings with the CN, strong absorption takes place in the inner region of the barrier. Then, the absorption probability at a given partial wave is equivalent to the condition of transmission through the barrier of the real part of the optical potential plus the centrifugal term. There are three main methods to calculate the absorption cross section.

Incoming wave boundary condition (IWBC). Within this model the imaginary part of the l-dependent potential in the radial equation is neglected. One uses the potential

$$U_l(r) = U_{\rm N}(r) + U_{\rm C}(r) + \frac{\hbar^2}{2\mu\, r^2}\, l(l+1). \tag{31}$$

The radial Schrödinger equations are then solved with incoming wave boundary condition at some internal radius, $R_{\rm in}$, which is usually the minimum of $U_l(r)$. This is equivalent to assuming total absorption once the flux from the elastic channel tunnels into the inner well of $U_l(r)$.

Wentzel, Kramers, Brillouin (WKB) method. In this procedure, which is an analytical representation of the IWBC model, the fusion cross section is represented as a sum of tunneling probabilities calculated by the WKB method [26].

Complex potential model. Here the Schrödinger equation is solved with the complex optical potential and the absorption cross section is then given by

$$\sigma_{\rm abs} = \frac{k}{E}\,\langle\psi^{(+)}| - W\,|\psi^{(+)}\rangle, \tag{32}$$

where

$$W(r) = {\rm Im}\{V_{\rm opt}\} \tag{33}$$

is the imaginary potential responsible for the absorption. The numerical calculations reported in the following rely on the partial wave decomposition of the Schrödinger equation, which leads to radial equations with the l-dependent potentials

$$V_l(r) = V_{\rm opt}(r) + \frac{\hbar^2}{2\mu\, r^2}\, l(l+1). \tag{34}$$

1. IWBC and semiclassical WKB method

The IWBC accounts for short-range absorption using a real potential in the radial equations but assuming that the incident wave is completely absorbed in the inner region of the barrier. On the other hand, absorption cross sections obtained with this quantum mechanical approach are very close to the ones obtained with the WKB method [27,28]. Both approaches are based on the implicit assumption that fusion is a tunneling phenomenon. The absorption cross section is given by the partial-wave expansion

$$\sigma_{\rm abs} = \frac{\pi}{k^2}\,\sum (2l+1)\,T(l,E), \tag{35}$$

where $T(l,E)$ is the absorption probability, which in the WKB method is equivalent to the transmission coefficient through the barrier of the potential of Eq. (31).

For simplicity, instead of Schrödinger equations with IWBC, we use Kemble's version of the WKB approximation, where the transmission coefficient is given by

$$T(l,E) = \frac{1}{1+\exp[2\,\Phi_l(E)]}, \tag{36}$$

with

$$\Phi_l(E) = \int_{r_1}^{r_2} k_l(r)\,dr. \tag{37}$$

Above,

$$k_l(r) = \frac{\sqrt{2\mu\,[E - U_l(r)]}}{\hbar} \tag{38}$$

is the local wave number and r_1 and r_2 are, respectively, the internal and the external turning points in the barrier region. In addition, there is an innermost turning point, $r_{\rm in}$, located in a region dominated by the centrifugal potential. The influence of this turning point is disregarded in the IWBC and the WKB descriptions of the collision. At energies above the barrier of the potential for the lth partial wave there are no real

values for the turning points r_1 and r_2. Then, keeping the integral of Eq. (37) along the real axis one gets $\Phi_l(E) = 0$, and thus $T(l, E) = 1/2$, for any energy above the barrier. This problem can be handled with the analytical continuation of the potential on the complex r plane [27,28]. The calculation of the transmission coefficient in this energy range can be simplified if one adopts the parabolic approximation for the potential barrier,

$$U_l(r) = B_l - \tfrac{1}{2}\,\mu\omega_l^2\,(r - R_l)^2, \tag{39}$$

where B_l, R_l, and $\hbar\omega_l$ are, respectively, the height, the radius, and the curvature parameter of the $U_l(r)$ barrier. In this case, the transmission coefficient can be evaluated analytically and one finds the so-called Hill-Wheeler transmission coefficient [29]

$$T^{\rm HW}(l, E) = \frac{1}{1 + \exp\left[2\pi\,(B_l - E)/\hbar\omega_l\right]}. \tag{40}$$

For low partial waves, the potential of Eq. (31) has a barrier with maximum B_l, located at R_l. The change of behavior takes place at the critical angular momentum, $l_{\rm cr}$, which is the l value satisfying the equation

$$\omega_l = \sqrt{-V_l''(R_l)/\mu} = 0. \tag{41}$$

The grazing energy for $l_{\rm cr}$, known as the critical energy and denoted by $E_{\rm cr}$, is then given by

$$E_{\rm cr} = B_{l_{\rm cr}}. \tag{42}$$

For $l > l_{\rm cr}$, the barrier disappears and $T(l, E)$ vanishes. Thus, according to Eq. (35), partial waves above $l_{\rm cr}$ do not contribute to $\sigma_{\rm F}$. Therefore, the partial-wave series is truncated at $l = l_{\rm cr}$. In this way, $\sigma_{\rm abs}(E > E_{\rm cr})$ decreases monotonically with E. Making the classical approximation for the transmission coefficient, $T(l < l_{\rm cr}, E > E_{\rm cr}) = 1$, the cross section above the critical energy takes the simple form

$$\sigma_{\rm abs}(E) \simeq \sigma_0 \times \frac{E_{\rm cr}}{E}, \tag{43}$$

with

$$\sigma_0 = \frac{\pi\hbar^2(l_{\rm cr} + 1)^2}{2\mu E}. \tag{44}$$

The above expression is very accurate, except for energies just above $E_{\rm cr}$ where the transmission coefficients for l just below $l_{\rm cr}$ are not yet very close to 1.

An important difference between absorption probabilities calculated using the complex potential method and in the WKB/IWBC approaches is that in the former there is an inherent wave reflection from the imaginary part of the potential. This reflection is an effective repulsion which renders the strength to be smaller than the announced one.

2. *Calculations with explicit use of imaginary potentials*

The treatment of absorption by IWBC or the WKB method can only be used to describe short-range absorption, corresponding to the fusion process. However, one frequently wants to make theoretical predictions of reaction cross sections with one-channel calculations. In such cases, absorption arises both from fusion and from direct reactions. One then solves the Schrödinger equation with a complex potential whose imaginary part has a longer range than in the case of pure fusion.

Thus, an important issue in quantum mechanical descriptions of scattering is the range of the imaginary potential. In coupled-channel calculations including all relevant direct channels, fusion is the only process the imaginary potential accounts for. In this case, the couplings act at very short distances, in the inner region of the Coulomb barrier. The same happens when the influence of direct channels is neglected. In such cases, the imaginary potential is usually represented by the Woods-Saxon function

$$W(r) \equiv W^{\rm F}(r) = \frac{W_0}{1 + \exp\left[(r - R_0)/a_0\right]}, \tag{45}$$

with

$$R_0 = r_0\left[A_{\rm P}^{1/3} + A_{\rm T}^{1/3}\right].$$

The condition of short-range strong absorption is guaranteed by a large strength parameter, say $W_0 = -50$ MeV, and small radius and diffusivity parameters, such as $r_0 = 1.0$ fm and $a_0 = 0.2$ fm.

On the other hand, in typical optical model analyses, elastic and total reaction cross sections of potential scattering calculations are compared with data. Of course, the experimental cross sections are influenced by both fusion and direct reactions. Thus, the imaginary potential must have a longer range, acting both in the inner region of the Coulomb barrier and in the barrier region. Then one may use a WS function with larger values of the r_0 and a_0 parameters, or another function with a similar range. Alternatively, one can use the same radial dependence of the real potential, and multiply the strength parameter by a factor λ slightly less than one. That is,

$$W^{\rm R}(r) = i\,\lambda\,U_{\rm N}(r), \tag{46}$$

where $U_{\rm N}(r)$ is the real part of the nuclear interaction. Gasques *et al.* [25] obtained good descriptions of data of a large number of systems using the above procedure. They adopted the São Paulo potential [11,30], with $\lambda = 0.78$.

D. Absorption vs fusion: CN formation probability

It is clear that fusion corresponds to absorption in the inner region of the potential barrier. However, short-range absorption does not necessarily mean fusion. The conditions for CN formation must be satisfied. Then, the fusion cross sections may be written as

$$\sigma_{\rm F} = \frac{\pi}{k^2}\sum(2l + 1)\,T(l, E)\,\mathcal{P}_{\rm CN}(l, E), \tag{47}$$

where $\mathcal{P}_{\rm CN}(l, E)$ is the CN formation probability. This probability depends on two contributing factors, which are discussed below.

The first factor is related to the density of states of the compound system, and their widths. The common assumption is that the probability of formation of the CN is unity, once the system overcomes the Coulomb barrier. Even at energies around the Coulomb barrier, the CN resonances are strongly overlapping and thus the system always finds a way to form

the CN. Thus, setting $\mathcal{P}_{\rm CN}(l, E) = 1$ is quite appropriate. Exceptions to this can be found in collisions of light systems at energies well below the Coulomb barrier, where the CN formation probability must be less than one. This probability depends on the product $\rho_{\rm CN} \times \Gamma_{\rm CN}$, where $\rho_{\rm CN}$ is the average density of states of the compound nucleus and $\Gamma_{\rm CN}$ is their average width. The average spacing between the resonances is $D_{\rm CN} = 1/\rho_{\rm CN}$. The CN formation probability is here taken to be given by the sum-over-resonances-based formula of Moldauer-Simonius (MS) [31–33],

$$\mathcal{P}_{\rm CN}^{(MS)}(l, E) = 1 - e^{-2\pi\alpha}, \tag{48}$$

with

$$\alpha = \Gamma_{\rm CN}(l, \varepsilon^*_{\rm CN}) \times \rho_{\rm CN}(l, \varepsilon^*_{\rm CN}), \tag{49}$$

where $\varepsilon^*_{\rm CN}$ is the CN excitation energy in a collision with energy E and angular momentum l. Above, $\rho_{\rm CN}(l, \varepsilon^*_{\rm CN})$ and $\Gamma_{\rm CN}(l, \varepsilon^*_{\rm CN})$ are, respectively, the corresponding density of states and their average width.

The factor $\mathcal{P}_{\rm CN}^{(MS)}(l, E)$ of Eq. (48) may be very important when $\alpha \ll 1$. Such a situation was discovered in the case of fusion of $^{12}C + ^{12}C$ at deep sub-barrier energies [34]. The authors of Ref. [34] found for $\mathcal{P}_{\rm CN}^{(MS)}(l, E)$ at these low energies, the value $\approx$0.8.

The second factor is that the projectile must remain close to the target for a long time, orders of magnitude longer than the time of transit. While the system stays in the inner region of the potential barrier, the kinetic energy of the relative motion is dissipated into intrinsic degrees of freedom, until the formation of an equilibrated CN. For this purpose it is necessary that the system be trapped in a neighborhood of the minimum of the potential $U_l(r)$. Clearly, this cannot happen at angular momenta higher than the critical value, $l_{\rm cr}$, above which $U_l(r)$ ceases to have a pocket.

As said above the hindrance factor given by the Moldauer-Simonius formula [Eq. (48)] is effective at low energies where the CN resonances are not overlapping. This factor is not expected to be important in the collisions studied in the present work and for this reason it will be assumed to be equal to one. On the other hand, the hindrance above the critical angular momentum depends exclusively on the real part of the optical potential, and is mostly related to the strong competition of direct reaction channels simulated by a stronger dynamic polarization potential.

The higher-energy (HE) CN hindrance factor, call it $\mathcal{P}_{\rm CN}^{(\rm HE)}(l, E)$, related to couplings to many inelastic channels and to the breakup channels (incomplete fusion), can be schematically accounted for in calculations with complex potentials,

$$\begin{aligned} \mathcal{P}_{\rm CN}^{(\rm HE)}(l, E) &= 1, \quad \text{for } l < l_{\rm cr} \\ &= 0, \quad \text{for } \geqslant l_{\rm cr}. \end{aligned} \tag{50}$$

We adopt this CN formation probability, $\mathcal{P}_{\rm CN}^{(\rm HE)}(l, E)$, namely the use of $l_{\rm cr}$ cutoff, in the applications of the next section. In this way, our fusion cross sections behave as in the Glas and Mosel [35] model (GM). These authors employ the WKB method for the tunneling probability and use an $l_{\rm cr}$ in the l sum

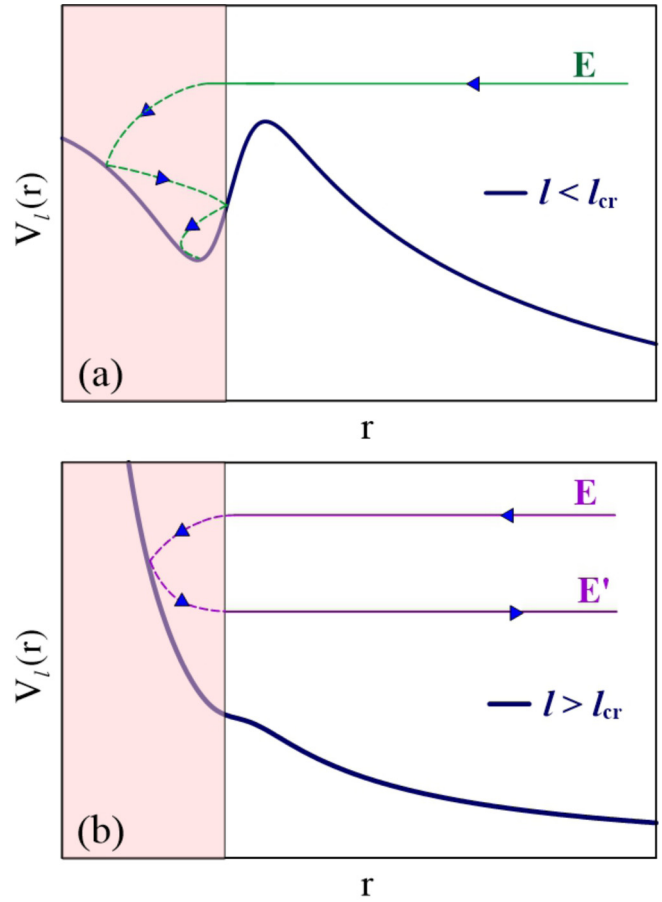

FIG. 1. Schematic representation of the dissipation of the incident energy. (a) shows a collision with $E > B_l$ and $l < l_{\rm cr}$, where it leads to the formation of a CN. (b) shows a collision with $E > E_{\rm cr}$ and $l > l_{\rm cr}$. In this case the system emerges with an energy $E' < E$, without forming a CN.

in their calculation of the fusion cross section at the higher energies. So in a way we are generalizing the GM model to the complex potential model. Figure 1 illustrates the dissipation of the kinetic energy of the projectile-target relative motion in two situation. Figure 1(a) shows a collision with angular momentum $l < l_{\rm cr}$, at an energy E satisfying the condition: $E_{\rm cr} > E > B_l$. As the system enters the strong absorption region, represented by a pink shaded area, the energy E is quickly dissipated and the system is caught in the pocket of the potential $U_l(r)$. Then, after a long time, the excitation energy of the system is fully thermalized and the CN is formed. In this collision the CN formation probability is equal to one.

A different situation is depicted on Fig. 1(b). Now the angular momentum is higher than $l_{\rm cr}$ and the collision energy is higher than $E_{\rm cr}$. As before, there is energy dissipation as the system reaches the strong absorption region. However, there is no CN formation. Owing to the strongly repulsive nature of $U_l(r)$ and to the absence of a pocket, the duration of the collision is far too short for full thermalization. Then, there is some dissipation of the incident energy and the collision partners may exchange a few nucleons, but they

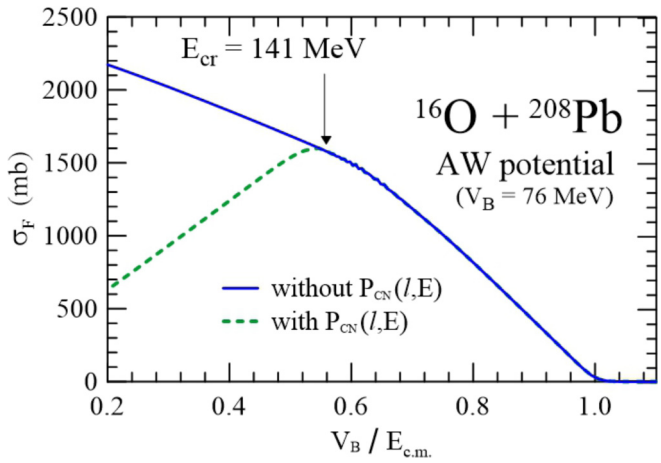

FIG. 2. Fusion cross sections for the $^{16}O + ^{208}Pb$ system calculated with the AW nuclear interaction and the short-range imaginary potential of Eq. (45), with parameters $W_0 = -50$ MeV, $r_0 = 1.0$ fm, and $a = 0.2$ fm. The blue solid line does not take into account the CN formation probability of Eq. (50) whereas the green dashed line does.

eventually reseparate, keeping their identities. Such processes correspond to multistep excitations and preequilibrium reactions. Thus, they are very important to the total reaction cross section but they do not contribute to fusion. In this case the CN formation probability is zero.

Figure 2 illustrates the importance of the CN formation probability in $^{16}O + ^{208}Pb$ fusion. The full blue curve represents the calculation without the l_{cr} cutoff while the dashed green one with the l_{cr} cutoff. The calculations were performed with the AW interaction plus the short-range imaginary potential of Eq. (45). For the latter, we adopted the parameters $W_0 = -50$ MeV, $r_0 = 1.0$ fm and $a = 0.2$ fm. Usually, fusion and reaction cross sections at energies reaching E_{cr} are plotted against the inverse of the energy. We use instead the dimensionless variable V_B/E. As expected, the two curves are indistinguishable at energies below E_{cr}, which corresponds to $V_B/E = 0.54$. This corresponds to collisions behaving as in Fig. 1(a). However, they are dramatically different above the critical energy and the difference increases with the energy. This corresponds to the situation of Fig. 1(b). Although the absorption increases with energy, the fusion cross section is proportional to $1/E$, following Eq. (43). We see from this calculation that the inclusion of the compound nucleus formation probability of Eq. (50) in the l sum, or equivalently the introduction of the l_{cr} cutoff in the said sum of the fusion cross section calculated with the complex potential model, reduces the cross section by as much as a factor of 4 at the highest energy considered in the figure.

III. APPLICATION TO HEAVY AND LIGHT SYSTEMS

In this section we investigate the influence of the treatment of absorption and the choice of the nuclear potential in fusion cross sections of a heavy ($^{16}O + ^{208}Pb$) and of a light ($^{6}Li + ^{12}C$) system.

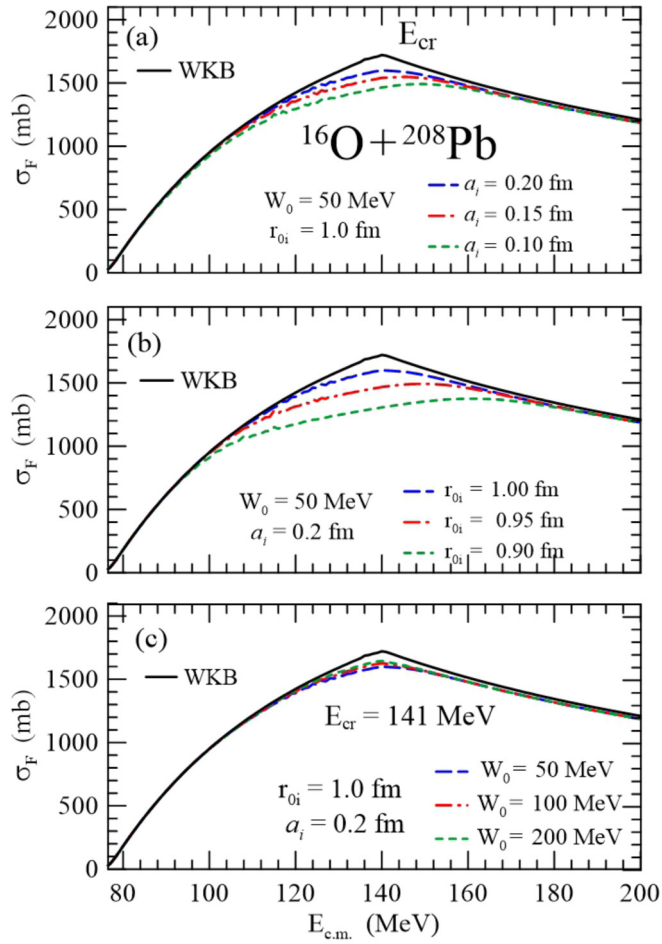

FIG. 3. Fusion cross sections for the heavy system, $^{16}O + ^{208}Pb$. (a) shows the dependence on the diffuseness parameter, (b) the dependence on the radius parameter, and (c) the dependence on the strength of the imaginary potential. The solid black line represents the calculation within the WKB theory. See text for details.

A. Dependence of σ_F on the treatment of absorption

Usually, it is assumed that heavy-ion fusion cross sections of barrier penetration models (IWBC or WKB) at near-barrier energies are equivalent to cross sections of quantum mechanical calculations with strong short-range imaginary potentials, such as WS potentials with parameters in the range: 50 MeV $\lesssim W_0 \lesssim$ 200 MeV, 0.9 fm $\lesssim r_0 \lesssim$ 1.0 fm and 0.1 fm $\lesssim a_0 \lesssim$ 0.2 fm. In this section, we check this assumption comparing cross sections for one heavy system and one light system. We use as benchmarks the cross sections of quantum mechanical calculations with WS imaginary potentials with the parameters $W_0 = 50$ MeV, $r_0 = 1.0$ fm and $a_0 = 0.2$ fm. In this comparison we adopt the Akyüz-Winther potential [13,36] for the real part of the nuclear interaction. With this choice, the Coulomb barriers for the $^{16}O + ^{208}Pb$ and $^{6}Li + ^{12}C$ systems are $V_B = 76.5$ and $V_B = 3.3$ MeV, respectively. The corresponding critical energies are $E_{cr} =$ 141 MeV and $E_{cr} = 21.1$ MeV. The fusion cross sections obtained with the different imaginary potentials and with the

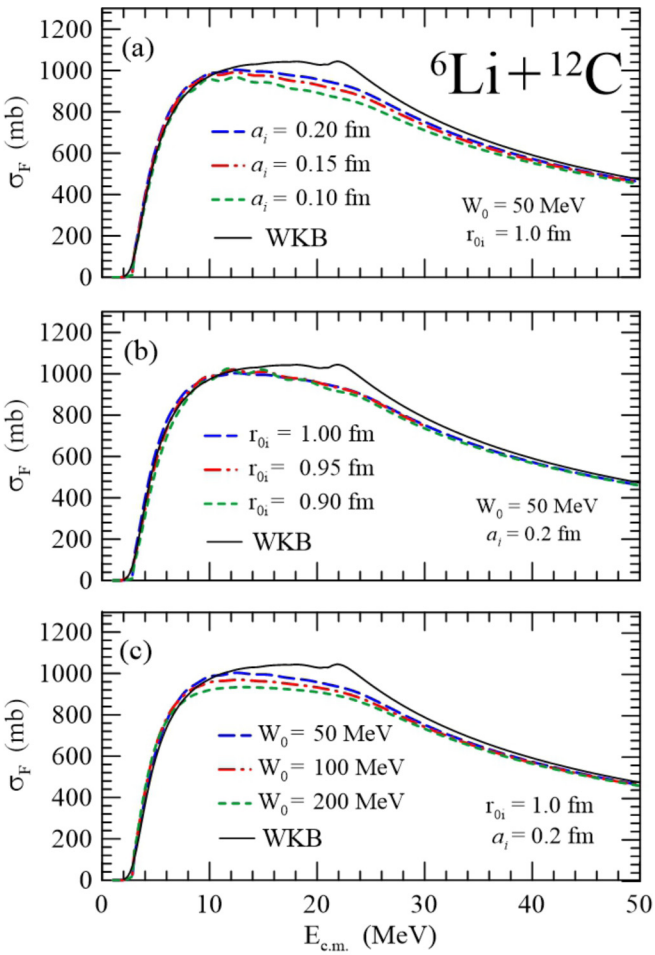

FIG. 4. Same as Fig. 3 for the light mass system, ^{6}Li + ^{12}C. See text for details.

WKB approximation for the two systems are shown in Figs. 3 and 4.

Figure 3 shows cross sections for the ^{16}O + ^{208}Pb system. Results of the WKB calculation, represented by black solid lines, and results of calculations with the imaginary WS potential with the benchmark parameters ($W_0 = -50$ MeV, $r_0 = 1.0$ fm, and $a_0 = 0.2$ fm), represented by blue dashed lines, are shown on the three panels of the figure. The remaining curves were obtained with other values of a_0 [Fig. 3(a)], other values of r_0 [Fig. 3(b)], and other values of W_0 [Fig. 3(c)].

At above-barrier energies below 100 MeV, the cross sections of all calculations are very close. At higher energies, the WKB cross section exceeds the ones obtained with the imaginary potentials, which differ among themselves. The discrepancies are maximal in the neighborhood of the critical energy, $E_{cr} = 141$ MeV. Beyond this value, the differences among the curves decrease, as they all exhibit the asymptotic behavior of Eq. (43). Comparing the curves on the three panels one concludes that the cross sections are more sensitive to the choice of r_0 than of the other two parameters. The results of a similar study for the light ^{6}Li + ^{12}C system are presented in Fig. 4. Although the trends of the fusion cross sections calculated within the WKB and absorption methods are approximately the same, the discrepancies now are slightly smaller than in the previous case. Further, we notice that dispersion among the cross sections obtained with imaginary potentials with different parameters is less pronounced than in the previous system, and now the sensitivity of the cross sections to changes in W_0 is larger that to those in r_0 or a_0.

We now try to give a qualitative interpretation of the energy dependence of σ_F. Near the Coulomb barrier, the number of partial waves contributing to fusion grows with E and, accordingly, the cross section increases monotonically. For a low partial wave, the effective potential has the shape represented on Fig. 1(a). The potential has a barrier, of height B_l, followed by a dip, as r decreases. For an energy $E_0 < B_l$, fusion is determined by the probability of tunneling trough the barrier. If tunneling occurs, then the fusion process takes place, as the system continues its motion drawn by the strong nuclear potential in the well, until it reaches the strong absorption region, indicated by the shaded band at the left of the figure. Then the CN is formed. The outcome is the same at an energy $E > B_l$. In this case the system overcomes the barrier and reaches the strong absorption region. There, the kinetic energy is completely dissipated and the system is caught in the dip of the potential. This situation is schematically represented on Fig. 1(a).

As the angular momentum increases, the repulsive centrifugal potential leads to a decrease in the depth of the effective potential well in the inner region of the Coulomb barrier, until, for $l = l_{cr}$, the potential has an inflection point instead of a barrier-well shape. The effective potential for a partial-wave above l_{cr} is represented on Fig. 1(b). For a high enough energy, E, the system overcomes the barrier and reaches the strong absorption region, where its kinetic energy is partly dissipated. However, there is no CN formation. The system re-separates with an energy E', lower than E. This process corresponds to the situation schematically represented on Fig. 1(b). As such, partial-waves above l_{cr} do not contribute to fusion. Accordingly the partial-wave series of Eq. (47) must be truncated at l_{cr}, which is guaranteed with our choice of $\mathcal{P}_{CN}(l, E)$ of Eq. (50). Then, the cross section at high energies ($E > E_{cr}$) decreases linearly with E, following Eq. (43). This behavior can be observed in Figs. 3 and 4.

Inspecting Figs. 3 and 4, one concludes that WKB cross sections are very close to the ones obtained by quantum mechanics with strong absorption potentials, at near-barrier energies and at energies well above E_{cr}. However, they differ at energies in the neighborhood of E_{cr}. Further, the quantum mechanical cross sections in this region depend on the parameters of the imaginary potential. The discrepancies in this energy range arise from reflections by the real and the imaginary parts of the potentials at partial waves just below l_{cr}. In this case there is a single turning point very close to the barrier radius, outside the region of strong absorption. Then the incident wave is reflected without contributing to fusion. WKB calculations neglect this effect and for this reason they overestimate the fusion cross section in the neighborhood of E_{cr}. At higher energies the situation is different. The turning point for that same partial wave moves into the strong absorption region, and then the fusion probability is close to one both in the WKB and in the quantum mechanical calculations.

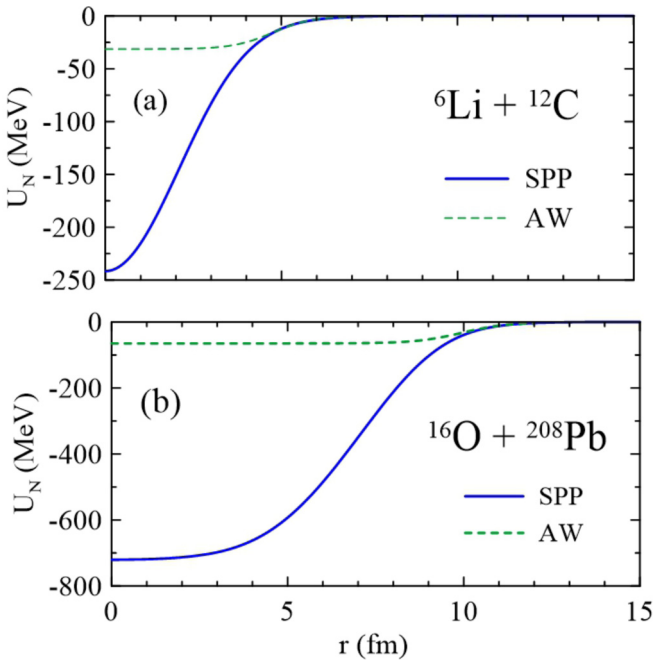

FIG. 5. The AW and the SPP potentials for the ^{6}Li + ^{12}C and ^{16}O + ^{208}Pb systems.

B. Dependence of σ_F on the nuclear potential

Now we investigate the sensitivity of the fusion cross sections to the choice of the nuclear potential. We study the ^{16}O + ^{208}Pb and ^{6}Li + ^{12}C systems, performing calculations with complex potentials. We consider the AW and the SPP nuclear interactions, and adopt the short-range imaginary potential of Eq. (45), with the parameters: $W_0 = 50$ MeV, $r_0 = 1.0$ fm and $a = 0.2$ fm.

Figure 5 illustrates the situation for these two bare nuclear potentials that coincide on the external region, but that have very different predictions for the inner well. Table I shows the heights, radii, and curvature parameters in the parabolic fits of the AW and SPP barriers. It shows also the critical energy in each case. As we have noticed, the barrier parameters for the two potentials are quite similar, for both systems. Further, the critical energies predicted by the two potentials for the light ^{6}Li + ^{12}C system are not very different. The one predicted by the SPP is roughly 25% higher. However, the critical energies for the heavy ^{16}O + ^{208}Pb system are, indeed, very different, with the prediction of the SPP being almost three times larger than the value predicted by the AW potential. The reason why the critical energies for the SPP are systematically higher is that this potential is much deeper than the AW. Whereas the depth of the former is of a few tens of MeV, that for the latter is a few hundreds of MeV. This difference becomes progressively more important as the mass of the system grows, as illustrated in Fig. 5. The critical energy determines the transition between two different energy regimes of the fusion cross section, referred to as region 1 (near barrier) and region 2 (above E_{cr}). Since this transition can be observed in the data, the experimental determination of the transition energy can be used as a criterion to select appropriate models for the bare potential. Having this in mind, we compare the cross sections calculated with the AW and the SPP potentials with available data. Figure 6 shows the comparison for the ^{16}O + ^{208}Pb system. The figure shows the AW cross section (green dashed line) in comparison with the SPP cross section (blue solid line) and the data of Morton *et al.* [37] (black open circles), and of Back *et al.* [38] (red squares). The data of Ref. [37] is restricted to the low-energy region, where the two theoretical curves are very close, and they agree very well with the theory. The older data of Ref. [38] reaches higher energies. Three data points were taken at energies below the critical energy for the two potentials and they are a little lower than the theoretical curves. The fourth data point was taken at an energy slightly higher than the critical energy of the AW potential, and it seems to follow the growing trend of the SPP cross section. However, considering that there is a single point in this region, the comparison of the data with the theoretical curves is not conclusive. Figure 7 shows an analogous comparison of cross sections for the ^{6}Li + ^{12}C system. The notation of the two

TABLE I. The parameters of the parabolic approximation for the Coulomb barriers of the systems considered in the present work. The corresponding critical energies are also shown.

System:	^{16}O + ^{208}Pb	^{6}Li + ^{12}C
V_B (MeV)		
AW:	76.5	3.3
SPP:	76.0	3.0
R_B (fm)		
AW:	11.6	7.4
SPP:	11.7	7.7
$\hbar\omega$ (MeV)		
AW:	4.5	2.7
SPP:	4.6	2.9
E_{cr} (MeV)		
AW:	141	21.1
SPP:	384	26.3

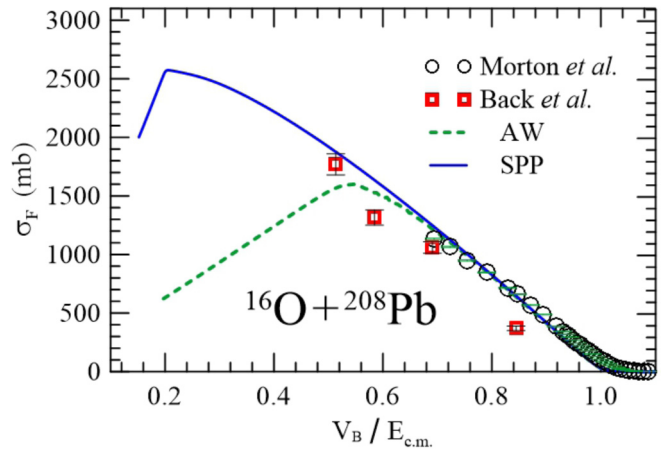

FIG. 6. Theoretical fusion cross sections for the ^{16}O + ^{208}Pb system, calculated with the AW (green dashed line) and the SPP (blue solid line). The experimental data of Morton *et al.* [37] (black open circles) and Back *et al.* [38] (red squares) are also shown.

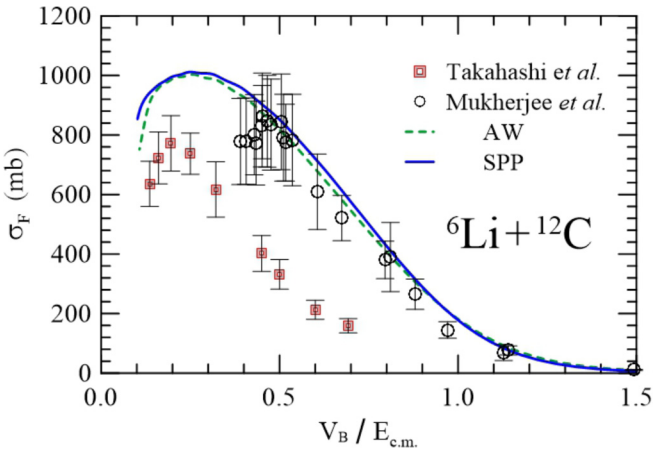

FIG. 7. Theoretical fusion cross sections for the $^6\mathrm{Li} + {}^{12}\mathrm{C}$ system compared with the available data. The notation of the curves is the same as in the previous figure and now the black open circles and the red square correspond respectively to the data of of Mukherjee *et al.* [39] and of Takahashi *et al.* [40].

curves is the same, whereas the black open circles and the red squares correspond, respectively, to the data of Mukherjee *et al.* [39] and Takahashi *et al.* [40]. First, one notices that the two curves are very close in the whole energy range. This is consistent with the similar barriers of the two potentials. The transition energies of the two potentials are also close. The data of Mukherjee *et al.* agree very well with the theoretical predictions of the two potentials. However, the data points at the highest energies seem to indicate a transition to region 2 before the theoretical predictions. Nevertheless they are still in agreement with the theoretical curves within the error bars. The data of Takahashi *et al.* are systematically lower than the theoretical curves, and also than the data of Mukherjee *et al.* On the other hand, they indicate a transition energy consistent with theoretical predictions.

IV. DISCUSSION AND CONCLUSIONS

We have presented a detailed investigation of the sensitivity of fusion cross sections to different commonly used nuclear potentials and treatments of absorption in potential scattering. An important general conclusion we have reached is that fusion cross sections can be computed with an optical potential as long as the range and the diffuseness of the imaginary part are small. Cross sections obtained in this way are practically the same as those with the incoming wave boundary condition as long as the incident energy is not too low.

We have evaluated fusion cross sections for the light $^6\mathrm{Li} + {}^{12}\mathrm{C}$ system and for the heavier $^{16}\mathrm{O} + {}^{208}\mathrm{Pb}$ system. We have performed calculations at energies ranging from the Coulomb barrier to beyond the critical energy. We have compared cross sections obtained within the WKB method with those obtained with optical model calculations with short-range absorption. We find that WKB cross sections are similar to the ones obtained from quantum mechanical calculations with different short-range strong absorption potentials, except in a neighborhood of the critical energy. In this region, the WKB cross sections are systematically higher than the quantum mechanical ones, which show some dependence on the parameters of the imaginary potential. We point out that in our optical model calculations the partial-wave series giving the fusion cross section must be truncated at the critical angular momentum, since higher partial waves do not contribute to fusion.

We have performed quantum mechanical calculations of fusion cross sections using different versions of the folding interaction: the Akyüz-Winther and the São Paulo potentials. The calculated cross sections were compared to each other and to the available experimental data. At near-barrier energies, the theoretical cross sections for the two methods are very close, and also close to most data. At higher energies, the situation for the $^6\mathrm{Li} + {}^{12}\mathrm{C}$ system did not change. However, the theoretical cross sections for $^{16}\mathrm{O} + {}^{208}\mathrm{Pb}$ were rather different. The AW cross section starts to decrease at $E = 141$ MeV ($V_B/E = 0.54$) whereas the one associated to the SPP keeps growing up to $E = 384$ MeV ($V_B/E = 0.20$). The difference is a consequence of the deeper well in the SPP, which leads to a higher critical energy. An important consequence is that one can obtain valuable information about the nuclear interaction at small distances comparing theoretical predictions with the data. Unfortunately, the presently available data for the $^{16}\mathrm{O} + {}^{208}\mathrm{Pb}$ system are restricted to the relatively low-energy region, where the two theoretical cross section are close. Therefore, experiments at higher energies should be important to help understand the nuclear potential between heavy ions at short separations.

ACKNOWLEDGMENTS

Work supported in part by the CNPq, CAPES, FAPERJ, FAPESP (Brazil), and by the PEDECIBA and ANII (Uruguay). The Brazilian authors acknowledge also partial financial support from the INCT-FNA (Instituto Nacional de Ciência e Tecnologia - Física Nuclear e Aplicações), research project 464898/2014-5.

[1] G. R. Satchler, *Direct Nuclear Reactions* (Oxford University Press, Oxford, 1983).
[2] H. Feshbach, *Theoretical Nuclear Physics: Nuclear Reactions* (Wiley Publishing, New York, 1992).
[3] I. J. Thompson and F. M. Nunes, *Nuclear Reactions for Astrophysics: Principles, Calculation and Applications* (Cambridge University Press, Cambridge, 2009), 1st ed.
[4] L. F. Canto and M. S. Hussein, *Scattering Theory of Molecules, Atoms and Nuclei* (World Scientific, Singapore, 2013).
[5] K. Hagino, N. Rowley, and A. T. Kruppa, Comput. Phys. Commun. **123**, 143 (1999).
[6] H. Feshbach, Ann. Phys. (N.Y.) **5**, 357 (1958).
[7] H. Feshbach, Ann. Phys. (N.Y.) **19**, 287 (1962).

[8] G. F. Bertsch, J. Borysowicz, H. McManus, and W. G. Love, Nucl. Phys. A **284**, 399 (1977).
[9] M. A. Cândido Ribeiro, L. C. Chamon, D. Pereira, M. S. Hussein, and D. Galetti, Phys. Rev. Lett. **78**, 3270 (1997).
[10] L. C. Chamon, D. Pereira, M. S. Hussein, M. A. Candido Ribeiro, and D. Galetti, Phys. Rev. Lett. **79**, 5218 (1997).
[11] L. C. Chamon, B. V. Carlson, L. R. Gasques, D. Pereira, C. De Conti, M. A. G. Alvarez, M. S. Hussein, M. A. Cândido Ribeiro, E. S. Rossi Jr., and C. P. Silva, Phys. Rev. C **66**, 014610 (2002).
[12] R. A. Broglia and A. Winther, *Heavy Ion Reactions* (Westview Press, Boulder, 2004).
[13] O. Akyüz and A. Winther, in *Nuclear Structure of Heavy Ion Reaction*, edited by R. A. Broglia, C. H. Dasso, and R. A. Ricci (North Holland, Amsterdam, 1981), Proc. E. Fermi Summer School of Physics.
[14] F. S. Levin and H. Feshbach, *Reaction Dynamics* (Gordon and Breach, New York, 1973).
[15] W. Hauser and H. Feshbach, Phys. Rev. **87**, 366 (1952).
[16] M. Kawai, A. K. Kerman, and K. W. McVoy, Ann. Phys. (N.Y.) **75**, 156 (1973).
[17] P. A. Moldauer, Phys. Rev. C **14**, 764 (1976).
[18] G. E. Mitchell, A. Richter, and H. A. Weidenmüller, Rev. Mod. Phys. **82**, 2845 (2010).
[19] W. Kretschmer and M. Wangler, Phys. Rev. Lett. **41**, 1224 (1978).
[20] J. J. M. Verbaarschot, Ann. Phys. (N.Y.) **168**, 368 (1986).
[21] M. M. Shalaby and G. R. Satchler, Nucl. Phys. A **442**, 469 (1985).
[22] C. J. Lin, H. M. Jia, H. Q. Zhang, F. Yang, X. X. Xu, F. Jia, Z. H. Liu, and K. Hagino, Phys. Rev. C **79**, 064603 (2009).
[23] V. Scarduelli, E. Crema, V. Guimarães, D. Abriola, A. Arazi, E. de Barbará, O. A. Capurro, M. A. Cardona, J. Gallardo, D. Hojman *et al.*, Phys. Rev. C **96**, 054610 (2017).
[24] I. J. Thompson, M. A. Nagarajan, J. S. Lilley, and M. J. Smithson, Nucl. Phys. A **505**, 84 (1989).
[25] L. R. Gasques, L. C. Chamon, P. R. S. Gomes, and J. Lubian, Nucl. Phys. A **764**, 135 (2006).
[26] L. F. Canto, P. R. S. Gomes, R. Donangelo, and M. S. Hussein, Phys. Rep. **424**, 1 (2006).
[27] A. J. Toubiana, L. F. Canto, and M. S. Hussein, Eur. Phys. J. A **53**, 34 (2017).
[28] A. J. Toubiana, L. F. Canto, and M. S. Hussein, Braz. J. Phys. **47**, 321 (2017).
[29] D. L. Hill and J. A. Wheeler, Phys. Rev. **89**, 1102 (1953).
[30] L. F. Canto, R. Donangelo, P. Lotti, and M. S. Hussein, J. Phys. G **23**, 1465 (1997).
[31] P. A. Moldauer, Phys. Rev. Lett. **19**, 1047 (1967).
[32] M. Simonius, Phys. Lett. B **52**, 279 (1974).
[33] P. A. Moldauer, Phys. Rev. C **11**, 426 (1975).
[34] C. L. Jiang, B. B. Back, H. Esbensen, R. V. F. Janssens, K. E. Rehm, and R. J. Charity, Phys. Rev. Lett. **110**, 072701 (2013).
[35] D. Glas and U. Mosel, Phys. Rev. C **10**, 2620 (1974); Nucl. Phys. A **237**, 429 (1975)
[36] R. A. Broglia and A. Winther, *Heavy Ion Reactions* (Westview Press, Boulder, 2004).
[37] C. R. Morton, A. C. Berriman, M. Dasgupta, D. J. Hinde, J. O. Newton, K. Hagino, and I. J. Thompson, Phys. Rev. C **60**, 044608 (1999).
[38] B. B. Back, R. R. Betts, J. E. Gindler, B. D. Wilkins, S. Saini, M. B. Tsang, C. K. Gelbke, W. G. Lynch, M. A. McMahan, and P. A. Baisden, Phys. Rev. C **32**, 195 (1985).
[39] A. Mukherjee, U. Datta Pramanik, S. Chattopadhyay, M. Saha Sakar, A. Goswami, P. Basu, S. Bhatacharya, S. Sen, M. L. Chatterjee, and B. Dasmahapatra, Nucl. Phys. A **635**, 305 (1998).
[40] J. Takahashi, M. Munhoz, E. M. Szanto, N. Carlin, N. Added, A. A. P. Suaide, M. M. de Moura, R. Liguori Neto, A. Szanto de Toledo, and L. F. Canto, Phys. Rev. Lett. **78**, 30 (1997).